

A Novel Delay-Doppler-Based Channel Estimation Method in Doubly-Dispersive OCDM Systems

Salah Eddine Zegrar^{ID}, *Graduate Student Member, IEEE*, and Hüseyin Arslan^{ID}, *Fellow, IEEE*

Abstract—Orthogonal chirp division multiplexing (OCDM) has recently emerged as a new candidate for the 6G waveform. In high-mobility wireless channels, the inseparability of the data symbols in both time and frequency domains makes channel estimation in OCDM-based wireless communication quite challenging. In this letter, we address this issue by investigating the representation of the OCDM waveform in the delay-Doppler domain in which we reveal that OCDM carriers exhibit a sparse representation. Building upon this observation, we propose a low-complexity channel estimation technique for OCDM systems. This technique involves designing pilots in the Fresnel domain and estimating the channel in the delay-Doppler domain. We evaluate the performance of the proposed channel estimation and demonstrate the superior performance of our approach, showcasing both high accuracy and low computational complexity.

Index Terms—OCDM, channel estimation, doubly-dispersive channel, Fresnel domain, delay-Doppler domain.

I. INTRODUCTION

RECENTLY, orthogonal chirp division multiplexing (OCDM) has emerged as a promising alternative waveform to conventional multicarrier modulation schemes. Unlike orthogonal frequency division multiplexing (OFDM) which modulates the data over complex sinusoidals, OCDM utilizes the discrete Fresnel transform (DFnT) to modulate data onto orthogonal complex linear chirps in the time domain, which have the ability to combat challenges associated with wireless channels [1]. For instance, by spreading data over the entire time and bandwidth of the signal, OCDM exhibits increased robustness against multipath propagation [2], and narrowband interference [3]. This is particularly beneficial for achieving reliable communication in complex and frequency-selective environments. Moreover, by leveraging the close relationship between the DFnT and the discrete Fourier transform (DFT), the compatibility of OCDM systems with OFDM can be achieved, enabling seamless integration of OCDM into existing OFDM-based communication systems and satisfying the crucial condition of backward compatibility [4].

The reliability of communications with OCDM highly depends on the accuracy of channel estimation, particularly in the presence of delay and Doppler spread. Yet, most existing works only consider the static channels to estimate

in OCDM systems without considering mobility [5], [6], [7] where pilots are embedded in the time or frequency domain. In [8], only a single frequency offset is considered when doing estimation in the Fresnel domain. On the other hand, for doubly selective channels, a basis expansion model (BEM) is adopted to characterize doubly selective channels in [9] using pilot chirp assisted (PCA)-OCDM systems. A method is developed to minimize the minimum mean squared error (MMSE) of the channel estimator. However, the complexity of the matrix inversion required in MMSE is $\mathcal{O}(N^3)$, which is highly complex and prohibitive for channels with long delays. Additionally, MMSE requires prior knowledge of channel statistics.

This letter derives the representation of the OCDM in the delay-Doppler domain, showing that each OCDM carrier has a sparse nature in the delay-Doppler lattice. Then, exploiting the sparse nature of the orthogonal chirps in both domains, this letter proposes a novel low-complexity channel estimation scheme for OCDM systems by designing the pilots in the chirp domain and estimating the channel in the delay-Doppler domain. The main contributions are summarized as follows¹:

- We derive the mathematical representation of OCDM carriers in the Zak-space and demonstrate that linear orthogonal chirps possess a sparse nature in the delay-Doppler lattice. Additionally, we establish that OCDM can be seen as a pre-processed delay-Doppler modulation and introduce a relationship between OCDM and the Orthogonal Time-Frequency Space (OTFS) modulation.
- We propose a novel low-complexity pilot-based channel estimation method for OCDM systems that exploits the sparse nature of the OCDM carriers in both delay-Doppler and Fresnel (chirp) domain. The proposed method offers enhanced flexibility by allowing the utilization of any channel estimation scheme developed for the delay-Doppler domain, depending on the capabilities and requirements of the users or transceivers.
- We assess the performance of the proposed channel estimation method by analyzing two metrics: normalized mean square error (NMSE) and bit error rate (BER) for OCDM systems. The simulations highlight the effectiveness of the proposed algorithm in achieving accurate channel estimation with low-complexity.

Manuscript received 23 October 2023; revised 26 November 2023; accepted 15 December 2023. Date of publication 19 December 2023; date of current version 8 March 2024. This work was supported by the Scientific and Technological Research Council of Turkey (TUBITAK) under Grant 120C142. The associate editor coordinating the review of this article and approving it for publication was Q. Guo. (Corresponding author: Salah Eddine Zegrar.)

The authors are with the Department of Electrical and Electronics Engineering, Istanbul Medipol University, 34810 Istanbul, Turkey (e-mail: salah.zegrar@std.medipol.edu.tr; huseyinarslan@medipol.edu.tr).

Digital Object Identifier 10.1109/LWC.2023.3344231

¹Notation: Bold uppercase **A**, bold lowercase **a**, and unbold letters A , a denote matrices, column vectors, and scalar values, respectively. $[\alpha]_{\beta}$ and $\lfloor \frac{\alpha}{\beta} \rfloor$ take modulo- β of α and the integer quotient of $\frac{\alpha}{\beta}$, respectively. $\delta(\cdot)$ denotes the Dirac-delta function. \subset , \mathbb{N} , and \mathbb{Z} denote the subset operator, natural, and integer number sets, respectively. The symbol j represents the imaginary unit of complex numbers with $j^2 = -1$.

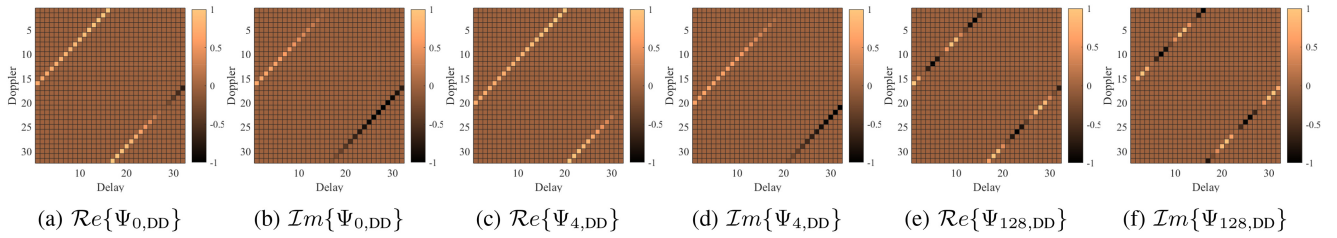


Fig. 1. The delay-Doppler representation of difference OCDM carriers with parameters: $L = 1$, $N_d = 32$, $M_d = 32$, $N = 1024$.

II. OCDM IN DELAY-DOPPLER DOMAIN

In this letter, we consider an OCDM transmission spanning a bandwidth B and time duration T , where a set of N orthogonal chirps are used to modulate N data symbols \mathbf{x} using the inverse discrete Fresnel transform (IDFnT). These N orthogonal chirp waveforms exhibit a linear frequency sweep over time and possess orthogonal properties, enabling them to be transmitted simultaneously without interference. The i -th ($i = 0, 1, \dots, N - 1$) OCDM carrier can be given as [1]

$$\psi_i(t) = e^{j\frac{\pi}{4}} e^{-j\pi\frac{N}{T^2}(t-i\frac{T}{N})^2}, 0 \leq t < T. \quad (1)$$

To facilitate practical implementation, the OCDM carriers in (1) are discretized by sampling them at times $t = m\frac{T}{N}$. This yields the discrete i -th OCDM carrier $\psi_i(m)$ given as

$$\psi_i(m) = e^{j\frac{\pi}{4}} e^{-j\pi\frac{(m-i)^2}{N}}, 0 \leq m < N. \quad (2)$$

A. OCDM Representation in Delay-Doppler Domain

The delay-Doppler domain serves as an intermediate representation between the time domain and the frequency domain. Let's suppose that the delay-Doppler grid is discretized into N_d delays and M_d Dopplers. Now, consider an arbitrary discrete sequence \mathbf{x} with a length of N points, where $N = M_d \times N_d = LN_d^2$, $M_d = LN_d$ and $L, N_d, M_d \in \mathbb{N}$. The discrete Zak transform (DZT), \mathbf{X}_{DD} , of \mathbf{x} is given by [10]

$$X_{DD}(k, l) = \frac{1}{\sqrt{N_d}} \sum_{n=0}^{N_d-1} x(k + nM_d) e^{-j2\pi\frac{l}{N_d}n}, \quad \text{for } 0 \leq k < M_d, 0 \leq l < N_d. \quad (3)$$

Computing $X_{DD}(k, l)$ requires obtaining M_d DFT operations of size N_d of the data sets $x(k), x(k + M_d), \dots, x(k + (N_d - 1)M_d)$ for $0 \leq k < M_d$. The sequence \mathbf{x} can be recovered from its DZT by the formula

$$x(k + nM_d) = \frac{1}{\sqrt{N_d}} \sum_{l=0}^{N_d-1} X_{DD}(k, l) e^{j2\pi\frac{l}{N_d}n} \quad \text{for } 0 \leq k < M_d, 0 \leq n < N_d. \quad (4)$$

The i -th OCDM carrier in (2) can be expressed as

$$\psi_i(k + nM_d) = e^{j\frac{\pi}{4}} W_N \left(-\frac{1}{2}(k + nM_d - i)^2 \right), \quad (5)$$

where $W_K(k) := e^{j2\pi k/K}$. Then, the DZT of ψ_i in (5) can be expressed as

$$\begin{aligned} \Psi_{i,DD}(k, l) &= \frac{1}{\sqrt{N_d}} \sum_{n=0}^{N_d-1} \psi_i(k + nM_d) W_{N_d}(nl) \\ &= \frac{\Omega_i}{\sqrt{N_d}} \sum_{n=0}^{N_d-1} W_{N_d}(\alpha n^2 + \beta_i n), \end{aligned} \quad (6)$$

where $\Omega_i := e^{j\frac{\pi}{4}} W_N(-(k - i)^2/2)$, $\alpha := -LN_d/2$, and $\beta_i := l + i - k$.

In order to assess the sparsity of OCDM carriers in the delay-Doppler domain, we show that if $\alpha + \beta_i \in \mathbb{Z}$, $\Psi_{i,DD}$ is only non-zero at M_d specific points within the delay-Doppler domain. Observe that since

$$W_{N_d}(\alpha n^2) = (-1)^{Ln^2} = (-1)^{Ln} = W_{N_d}(\alpha n), \quad (7)$$

then, we can write

$$\Psi_{i,DD}(k, l) = \frac{\Omega_i}{\sqrt{N_d}} \sum_{n=0}^{N_d-1} W_{N_d}((\alpha + \beta_i)n), \quad (8)$$

provided $L \in \mathbb{Z}$. It follows that $\Psi_{i,DD}(k, l)$ is sparse, i.e.,

$$\Psi_{i,DD}(k, l) = \begin{cases} \sqrt{N_d}\Omega_i, & [\alpha + \beta_i]_{N_d} = 0 \\ 0, & \text{otherwise} \end{cases}. \quad (9)$$

Fig. 1 provides an illustrative example of OCDM carriers exhibiting a sparse representation in the delay-Doppler domain. Specifically, Fig. 1(a-f) showcases the real and imaginary parts of the 0-th, 4-th, and 128-th OCDM carriers, respectively. Fig. 1(a-b) demonstrate that the root (i.e., 0-th) OCDM carrier of length $N = N_d \cdot M_d$ can be represented by N_d points in the delay-Doppler domain. Furthermore, Fig. 1(c-d) reveal that the 4-th OCDM carrier is essentially a shifted version of the 0-th carrier in the delay-Doppler domain. It is important to note that the OCDM carriers having index greater than N_d are the same with the root OCDM carrier shifted by $[i]_{N_d}$ changing its complex coefficient values. This is clearly depicted in Fig. 1(e-f), where $\hat{i} = [128]_{32} = 0$. Therefore, an OCDM in delay-Doppler domain consists of M_d non-overlapping orthogonal signals (shifted in delay and Doppler) each having N_d overlapping orthogonal signals.

B. OCDM as Precoded-OTFS

As demonstrated in Section II-A, we conclude that each OCDM carrier can be presented as a precoded sparse delay-Doppler signal as given in (9). Therefore, OCDM will fully populate an $M_d \times N_d$ delay-Doppler grid with $M_d \times N_d$ OCDM carriers as follows

$$X_{DD}^{\text{OCDM}}(k, l) = \sum_{i=0}^{M_d N_d - 1} \Psi_{i,DD}(k, l). \quad (10)$$

Then, OCDM can be seen as a pre-processed OTFS modulation [11]. This feature is exploited in the following section to design a novel channel estimation method for the OCDM signal where channel estimation pilots are designed in the chirp domain and the estimation is performed in the delay-Doppler domain.

III. PROPOSED OCDM CHANNEL ESTIMATION

The discrete time-domain OCDM signal is given as [1]

$$s(n) = e^{j\frac{\pi}{4}} \frac{1}{\sqrt{N}} \sum_{m=0}^{N-1} x(m) e^{-j\frac{\pi}{N}(m-n)^2} \quad (11)$$

Let $h(n)$ be a doubly-dispersive channel with the following time response

$$h(n) = \sum_{i=0}^{P-1} h_i \delta(n - l_i) e^{j\frac{2\pi k_i}{N}(n-l_i)}, \quad (12)$$

where P , h_i , l_i , and k_i denote the number of propagation paths, the channel gain, the integer delay, and Doppler shift of the i -th reflector, respectively. After the transmitted signal passes through the wireless channel, the received signal is found as

$$r(n) = \sum_{i=0}^{P-1} h_i s(n - l_i) e^{j\frac{2\pi k_i}{N}(n-l_i)} + w(n), \quad (13)$$

where $w(n)$ represents the additive white Gaussian noise (AWGN) with variance σ^2 . By applying the DFNT we get the received signal in the Fresnel Domain as follows

$$\begin{aligned} y(m) &= e^{-j\frac{\pi}{4}} \sqrt{N} \sum_{n=0}^{N-1} r(n) e^{j\frac{\pi}{N}(m-n)^2} + w(m) \\ &= \sum_{i=0}^{P-1} h_i e^{j\frac{\pi}{N}(m^2 - ([m-l_i-k_i]_N)^2)} \\ &\quad \times e^{-j\frac{2\pi}{N}(\frac{l_i^2}{2} + l_i[m-l_i-k_i]_N + k_i l_i)} \\ &\quad \times x([m-l_i-k_i]_N) + w(m). \end{aligned} \quad (14)$$

By simplifying (14), we find

$$y(m) = \sum_{i=0}^{P-1} \tilde{h}_i e^{j\frac{2\pi}{N} k_i (m - [l_i + k_i])} x([m - l_i - k_i]_N) + w(m), \quad (15)$$

where $\tilde{h}_i = h_i e^{j\pi \frac{k_i^2}{N}}$.

We propose a novel pilot design-based channel estimation in which N_p pilot symbols are distributed in the Fresnel domain such that they are overlapping orthogonally in delay-Doppler domain (i.e., $\hat{i} = [i]_{N_d}$ as depicted in Fig. 1). In order to be able to estimate the channel, the combination of these N_p pilots in delay-Doppler domain must be sparser and their spacing must be larger than the maximum delay l_{\max} and Doppler spreads k_{\max} , respectively. Therefore, the number of pilots should be $N_p \geq \max(l_{\max}, k_{\max})$.

Using the previous results, consider N_p pilots $x_p(m_p) = \sqrt{E_p} \delta(m - m_p)$ where E_p and m_p denote the power and location of the pilots, respectively. The pilots are transmitted within the data frame, and guards are added to eliminate interference from the data after passing through the wireless channel, as depicted in Fig. 2. The proposed OCDM frame along with the pilot, guard, and data symbol arrangements in the Fresnel domain is given as

$$x(m) = \begin{cases} x_p, & [m]_{\frac{N}{N_p}} = 0 \ \& \ m_p = l_p + \lfloor \frac{m N_p}{N} \rfloor \\ 0, & [m]_{\frac{N}{N_p}} = 0 \ \& \ m_p - l_G \leq m \leq m_p + l_G, \\ \sqrt{E_s} x_d, & \text{otherwise} \end{cases} \quad (16)$$

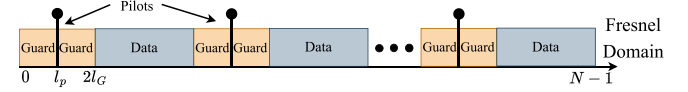
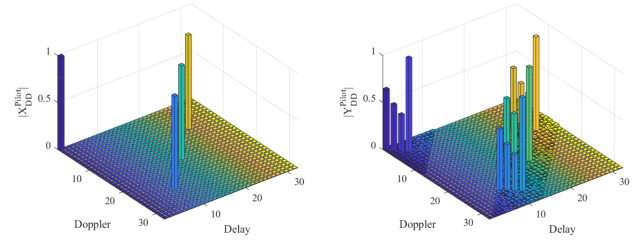


Fig. 2. Pilot, guard, and data symbol arrangement.



(a) Transmitter side.

(b) Receiver side.

Fig. 3. The delay-Doppler representation of proposed pilot signal with parameters: $N_p = 8$, $N = 1024$, $l_p = 16$, and $l_{\max} = k_{\max} = 4$.

Algorithm 1: The Proposed Channel Estimation

Input: Received signal $y(m)$

Output: l_i , k_i , and h_i .

- 1 Extract the pilot signal \mathbf{y}_p from \mathbf{y} in Fresnel domain as follows: $y_p(m) = y(m)$ for $m_p \leq m \leq m_p + l_G \forall m_p$;
 - 2 Transform \mathbf{y}_p to time domain and then to delay-Doppler domain and get Y_{DD}^{Pilot} as in Fig. 3(b);
 - 3 Apply threshold-based pilot detection to the received pilot signal as in [12];
 - 4 Estimate the channel parameters l_i , k_i , and h_i using threshold detection.
-

where $l_p \in [0, \frac{N}{N_p} - 1]$, $l_G = 2k_{\max} + l_{\max}$ gives the guard length, respectively. E_s denotes the average data symbol energy. Thus, the equivalent pilot symbols in delay-Doppler domain can be given as

$$X_{DD}^{\text{Pilot}}(k, l) = \sum_{i=0}^{N_p-1} \Psi_{l_p+i\frac{N}{N_p}, DD}(k, l). \quad (17)$$

Fig. 3 illustrates the pilot signal in the delay-Doppler domain before and after passing through the channel. To estimate the channel accurately in the delay-Doppler domain, we can employ any channel estimation technique designed for OTFS systems. In this letter, we adopt a threshold-based estimation approach inspired by the work conducted in [12]. The channel estimation framework is summarized in Algorithm 1.

IV. SIMULATIONS AND RESULTS

In this section, we conduct an evaluation of various aspects, including the computational complexity, the NMSE of the estimated doubly-dispersive channel, and the BER of the proposed OCDM system. quadrature phase shift keying (QPSK) modulation is used in the simulations, employing a frame size of $N = 1024$ and a delay-Doppler grid size of $M_d \times N_d = 32 \times 32$. For modeling the channel, we adopt the extended vehicular A model (EVA) [12], wherein the maximum delay-Doppler spread is $l_{\max} = k_{\max} = M_d/4 = 8$. Then, the number of pilots utilized in our scheme is $N_p = 8$.

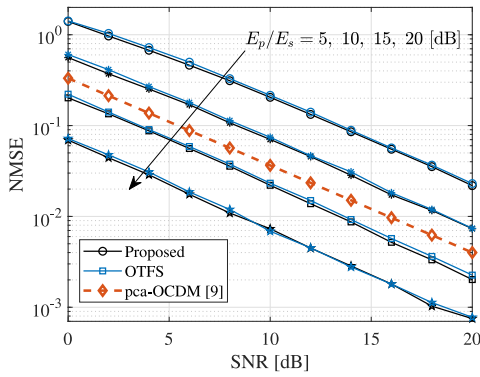


Fig. 4. Channel NMSE performance for different E_p/E_s values.

In this letter, we adopt the number of complex multiplications as a metric for assessing computational complexity. In the proposed method, the DFT can be efficiently implemented using the split-radix fast Fourier transform (FFT) algorithm, which requires approximately $\frac{N}{3} \log_2(N)$ complex multiplications for an N -point DFT when N is a power of 2 [13]. As described in Section III, the computational operations involved in our proposed method primarily revolve around converting the received signal to the time domain. This conversion requires performing the Fresnel transform, which consists of an N -point FFT and $2N$ element-wise multiplications. Subsequently, the time domain signal is transformed to the delay-Doppler domain using an N_d -point FFT. Note that step 3 and 4, in Algorithm I, have negligible computational complexity; therefore, they can be ignored. Based on these considerations, the total computational complexity of our proposed scheme can be expressed as $\mathcal{O}(\frac{N}{3} \log_2(N) + 2N + \frac{N_d}{3} \log_2(N_d))$. It is important to note that our proposed estimation scheme exhibits low computational complexity, particularly when compared to the PCA-OCDM method. The PCA-OCDM method employs the MMSE estimator, which has a significantly higher computational complexity proportional to $\mathcal{O}(N^3)$.

The NMSE performance of the proposed channel estimation technique is assessed and compared to the PCA-OCDM scheme, as illustrated in Fig. 4. The results demonstrate that the performance of our estimator improves with increasing pilot power E_p/E_s , where SNR in Fig. 4 represents the SNR of the data. Notably, our proposed scheme exhibits superior performance compared to the PCA-OCDM method presented in [9] when E_p/E_s almost exceeds 13 dB. It is worth mentioning that our proposed channel estimation scheme offers greater flexibility by allowing the utilization of any channel estimation scheme developed for the delay-Doppler domain depending on the users/transceivers capabilities and requirements, while achieving the same performance as OTFS channel estimation.

The results of BER are illustrated in Fig. 5, showcasing the implementation of zero-forcing (ZF) and MMSE detectors for symbol detection. The results indicate that when $E_p/E_s > 13$ dB, the proposed method outperforms the PCA-OCDM technique in [9]. This can be attributed to the higher accuracy of the estimated channel in the proposed method. It is also seen that OTFS performs better than the OCDM under perfect channel estimation. Also, note that the MMSE detector

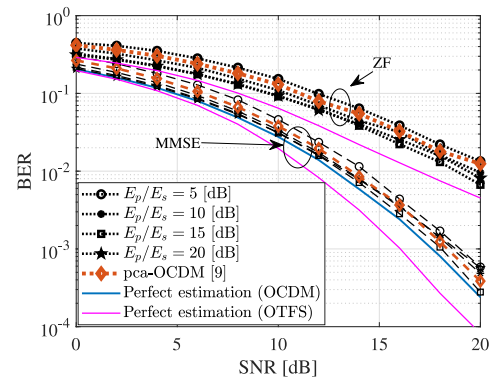


Fig. 5. The BER performance for different E_p/E_s values.

exhibits superior performance compared to the ZF due to its utilization of noise statistics in the detection process.

V. CONCLUSION

This letter presents a novel embedded pilot-aided OCDM channel estimation scheme. In the Fresnel domain, the arrangement of pilot, guard, and data symbols is specifically designed to mitigate interference between pilot and data symbols. The pilots are designed to exhibit sparsity in the delay-Doppler domain by leveraging the inherent characteristics of OCDM signaling as a precoded OTFS. Then, this letter presents a novel approach to accurately estimate doubly-dispersive channels in the delay-Doppler domain, while ensuring minimal computational cost.

REFERENCES

- [1] X. Ouyang and J. Zhao, "Orthogonal chirp division multiplexing," *IEEE Trans. Commun.*, vol. 64, no. 9, pp. 3946–3957, Sep. 2016.
- [2] M. S. Omar and X. Ma, "Performance analysis of OCDM for wireless communications," *IEEE Trans. Wireless Commun.*, vol. 20, no. 7, pp. 4032–4043, Jul. 2021.
- [3] M. S. Omar and X. Ma, "The effects of narrowband interference on OCDM," in *Proc. IEEE 21st Int. Workshop Signal Process. Adv. Wireless Commun. (SPAWC)*, 2020, pp. 1–5.
- [4] X. Lv, J. Wang, Z. Jiang, and W. Wu, "A joint radar-communication system based on OCDM-OFDM scheme," in *Proc. Int. Conf. Microw. Millim. Wave Technol. (ICMMT)*, 2018, pp. 1–3.
- [5] X. Wang, X. Shen, F. Hua, and Z. Jiang, "On low-complexity MMSE channel estimation for OCDM systems," *IEEE Wireless Commun. Lett.*, vol. 10, no. 8, pp. 1697–1701, Aug. 2021.
- [6] M. S. Omar and X. Ma, "Pilot symbol aided channel estimation for OCDM transmissions," *IEEE Commun. Lett.*, vol. 26, no. 1, pp. 163–166, Jan. 2021.
- [7] L. G. De Oliveira et al., "Discrete-Fresnel domain channel estimation in OCDM-based radar systems," *IEEE Trans. Microw. Theory Techn.*, vol. 71, no. 5, pp. 2258–2275, May 2023.
- [8] R. Zhang, Y. Wang, and X. Ma, "Channel estimation for OCDM transmissions with carrier frequency offset," *IEEE Wireless Commun. Lett.*, vol. 11, no. 3, pp. 483–487, Mar. 2022.
- [9] Y. Wang, R. Zhang, L. Yan, and X. Ma, "Pilot chirp-assisted OCDM communications over time-varying channels," *IEEE Wireless Commun. Lett.*, vol. 12, no. 9, pp. 1578–1582, Sep. 2023.
- [10] F. Lampel, A. Avarado, and F. M. J. Willems, "On OTFS using the discrete Zak transform," in *Proc. IEEE Int. Conf. Commun. Workshops (ICC Workshops)*, 2022, pp. 729–734.
- [11] R. Hadani and A. Monk, "OTFS: A new generation of modulation addressing the challenges of 5G," 2018, *arXiv:1802.02623*.
- [12] P. Raviteja, K. T. Phan, and Y. Hong, "Embedded pilot-aided channel estimation for OTFS in delay-Doppler channels," *IEEE Trans. Veh. Technol.*, vol. 68, no. 5, pp. 4906–4917, May 2019.
- [13] J. G. Proakis, "Signal analysis with higher order spectra," in *Advanced Digital Signal Processing*. New York, NY, USA: Macmillan, 1992.